JOURNAL OF MATERIALS SCIENCE 29 (1994) 4962–4966

Evidence of hexagonal diamond in plasma-deposited carbon films

S. R. P. SILVA, G. A. J. AMARATUNGA
Department of Engineering, Cambridge University, Trumpington Street, Cambridge CB2 1PZ, UK

E. K. H. SALJE
Department of Earth Science, Cambridge University, Cambridge CB2 3EQ, UK

K. M. KNOWLES
Department of Material Science and Metallurgy, Cambridge University, Cambridge CB2 3QZ, UK

Hexagonal diamond grains of ~30 nm diameter together with graphite and SiC are seen in predominantly amorphous carbon films deposited at low temperature on Si substrates from a CH_4 plasma vapour source. The different crystalline phases are identified by grazing-angle X-ray diffraction which allows for substrate rotation and tilting to enable the 2θ peaks to be correlated with the angular displacements of specific planes. Electron energy-loss spectroscopy shows the chemical composition of the films to be predominantly carbon with traces of oxygen. Raman spectroscopy shows the peaks to be associated with amorphous carbon and graphite, together with a peak at 1170 cm^{-1} which is attributed to microcrystalline hexagonal diamond.

1. Introduction

In the work of Bundy and Kasper [1] on synthetic diamond produced at high temperature and high pressure (HTHP), they found that in addition to conventional cubic diamond, hexagonal diamond was also formed by subjecting graphite to high pressures along its *c* axis. This type of "shock-compressed" diamond had previously been seen only in meteorites [2]. In this paper we report evidence for hexagonal diamond microcrystals in carbon films deposited on Si substrates using a low pressure, low temperature radio-frequency plasma-enhanced chemical vapour deposition (PECVD) process, where the d.c. self-bias between the plasma and substrate gives rise to ion acceleration.

Though deposition of cubic polycrystalline diamond films from a gas-phase hydrocarbon plasma at pressures around 10 torr and temperatures around 800°C is now well established, hexagonal diamond has not been observed in these films. Such films, which can be almost entirely composed of cubic polycrystalline diamond, are in essence formed by a chemical process due to the high substrate temperature activating surface reactions involving energetic CH_x^+ and H^+ radicals in the plasma. The other class of carbon films are those which are formed by a physical process where carbon and hydrocarbon ions are accelerated to 20–1000 eV and impinge on a substrate kept at low temperature. In these films cubic diamond has been observed as small microcrystallite inclusions in an amorphous carbon matrix. There are a number of reports on nucleation of diamond microcrystallites in an amorphous carbon matrix at low temperatures and at low pressures [3–7]. In all the reported cases the diamond nucleates as isolated clusters of crystals in a predominantly amorphous carbon matrix.

It is in the films which have been formed under PECVD conditions similar to those in a physical ion acceleration process that the hexagonal diamond microcrystals discussed were observed. These results provide evidence for the nucleation of hexagonal diamond at low temperature, as well as the identification of this material by a Raman peak seen previously on carbon films, but not identified as belonging to microcrystalline hexagonal diamond. Taking these results together with two recent reports of hexagonal diamond in plasma-deposited films [8, 9] we suggest that conditions for shock compression which lead to the formation of hexagonal diamond also exist during film growth utilizing accelerated ions from a plasma source.

2. Experimental procedure

Carbon films were deposited from a CH_4 (8%) Ar plasma, with the sample placed on the lower electrode. The flow rate of the composite gases was kept at a constant 160 sccm. The plasma was produced using a 13.56 MHz radio frequency (r.f.) power supply. A d.c. self-bias voltage of - 140 V was developed across the sheath space during deposition. The deposition pressure was 1 torr and the substrates were Si {1 0 0}. The lower electrode was cooled so that the temperature of the sample surface was kept below 120°C during the

0022–2461

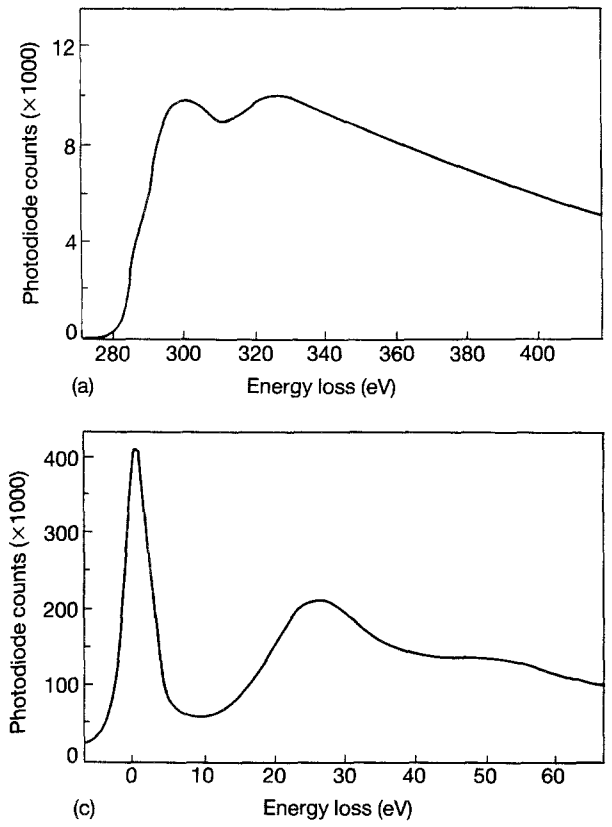

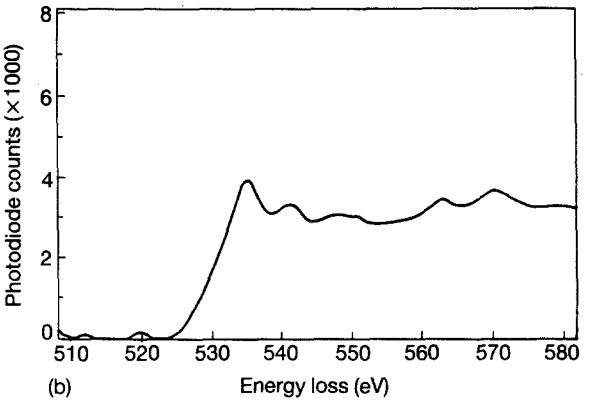

Figure 1 Electron energy-loss spectra for the carbon films showing (a) the carbon K edge, (b) the oxygen K edge and (c) the low-loss plasmon energy peak.

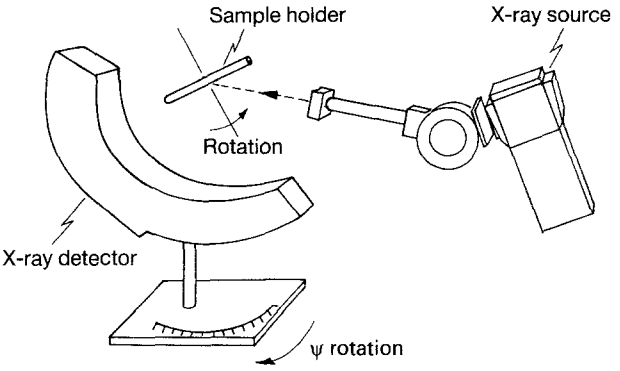

Figure 2 Schematic diagram of the X-ray diffraction system used.

deposition process. Although on a macroscopic scale the surface temperature recorded is small, on an atomic scale the thermal spikes created in ion collisions are expected to create an environment similar to a high temperature–high pressure process. In a model proposed by Weissmantel [10] thermal spikes created by the impinging ionic species collapse in time intervals of the order of 10^{-11} s and create non-equilibrium conditions suitable for the nucleation of diamond. The carbon films examined in this paper were deposited for 3 h, giving a final thickness of ~ 3 μm.

3. Results and discussion

The large thickness of the carbon films made the use of transmission electron microscopy to observe crystallinity in the film non-viable. But, by examining the thinner regions at the edges of the sample it was possible to obtain an electron energy-loss spectrum (EELS) of the sample which indicated the chemical composition to be predominantly carbon with traces of oxygen. By deconvoluting the K-edge spectra and comparing scattering cross-sections of each element it is possible to estimate the chemical composition of the amorphous carbon film. This reveals the films to be 95% carbon and 5% oxygen (Fig. 1a and b). The low-loss plasmon peak at 25.9 eV (Fig. 1c) is indicative of a dense amorphous carbon film.

X-ray analysis of the films was performed on a special apparatus using a CuK_α X-ray source operating at 600 W (Fig. 2). This system allows for the observation of diffraction intensity with independent θ, ψ and ρ scans. In plane ($\psi = 0°$), as well as out of plane ($\psi \neq 0°$), $\theta - 2\theta$ scans were performed where ψ is the angle of the detector relative to the forward diffraction. Peaks were located on the X-ray diffractometer by moving the detector systematically in angular steps of 5° away from $\psi = 0°$, with the X-rays always impinging on the sample at the lowest available grazing angle, y, of 4°. The X-ray detector was moved through ψ angle values ranging from 0 to 65°. At any given $\psi(\psi \neq 0°)$ the thin-film sample was rotated about its normal (angle ρ in Fig. 2) to detect diffraction peaks on the X-ray detector at (say) angles of γ. Peaks found in this manner can be related to the Bragg diffraction angle θ using the formula [11]

$$\cos 2\theta = \cos\psi \cos\gamma$$

where γ is the peak position on the detector for a given ψ. The X-ray diffraction peaks were transferred to a stereographic projection (i.e. $\psi = 0$, $\rho = 0$) using the rotational data of the sample positions (ρ) when maximized for a particular peak. The X-ray peak intensities obtained are small compared with single-crystal or polycrystalline films, but quite distinct when compared with the background intensities. When this technique is applied to (1 0 0) oriented single-crystal Si and Si powder standards the results obtained are in good agreement with those expected. These diffraction and Raman experiments were done without removal of the films from the substrate. Raman analysis on the films was carried out using a 514.5 nm laser focused in a micro-line.

Using this method to locate diffraction peaks at different detector positions has the advantage of

TABLE I X-ray peak assignment

d_{obs} (nm)	Graphite (a = 0.246 nm, c = 0.671 nm)		Hexagonal diamond (a = 0.252 nm, c = 0.412 nm)		SiC (4H) (a = 0.308 nm, c = 0.505 nm)		Cubic diamond (a = 0.357 nm)	
	d (nm)	hkl	d (nm)	hkl	d (nm)	hkl	d (nm)	hkl
0.334	**0.336**	**(0 0 2)**						
0.218	0.213	(1 0 0)	**0.218**	**(1 0 0)**				
0.208	0.203	(1 0 1)	**0.206**	**(0 0 2)**	0.209	(1 0 3)	0.206	(1 1 1)
0.197			**0.193**	**(1 0 1)**				
0.182	**0.180**	**(1 0 2)**					0.179	(2 0 0)
0.168	**0.168**	**(0 0 4)**						
0.160					**0.161**	**(1 0 5)**		
0.154	**0.154**[a]	**(1 0 3)**	0.150	(1 0 2)	**0.154**[a]	**(1 1 0)**		
0.141					**0.142**	**(1 0 6)**		
0.129					**0.129**	**(2 0 2)**		
0.126			**0.126**[b]	**(1 1 0)**			0.126	(2 2 0)
	0.123[b]	**(1 1 0)**						
0.119	0.116	(1 1 2)	**0.116**	**(1 0 3)**				

[a] X-ray data match angles between planes and 2θ peak (approximate) for both SiC and graphite.
[b] X-ray data match angles between planes and 2θ peak (approximate) for both graphite and hexagonal diamond.

enabling the identification of different crystalline components with different orientations in mixed-phase films such as the carbon films studied. The preservation of interplanar spacings and therefore θ from a given crystal as the detector is moved through ψ is seen as a shift in the position of γ of the detected X-ray peaks. By plotting these shifts on a stereographic projection for different detector angles (and rotations), it is possible to identify the different crystalline components and their orientation with respect to the film surface. For example it is possible using this method to distinguish whether an X-ray peak at a 2θ Bragg angle of 44° is due to the presence of (say) the (1 1 1) diamond or the (1 0 1) graphite planes [12].

The position of ψ and ρ which would be required for a shift in the detected X-ray peak to a defined position γ on the X-ray detector corresponding to the crystal planes of cubic diamond and hexagonal graphite can be calculated. By the systematic variation of ψ and ρ it is possible to verify whether X-ray peaks detected at new γ positions correspond to those of diamond or graphite. Distinction between the crystal types with different orientations which may give similar Bragg diffraction angles for some planes is therefore possible. Sets of diffracting peaks (Fig. 3) which preserve an angular relation corresponding to specific hexagonal planes are shown as a and b, b and c, c and d, d and e, e and f, g and h, i and j. The angular relationship between these hexagonal diamond planes can be obtained from the intersections on great circles and are 58°, 75°, 75°, 32°, 62°, 32° and 32°, respectively. Diffraction from all possible planes in a particular crystal cannot be detected to form an angularly closed pattern due to restrictions in the geometry of the X-ray apparatus, and the low intensity of diffraction from certain planes (the crystals are embedded in an amorphous matrix). Similar stereographic projections were obtained from the same film corresponding to diffraction peaks which could be assigned to graphite and 4H SiC. When X-ray 2θ peaks that could be due to cubic diamond were transferred to a stereographic

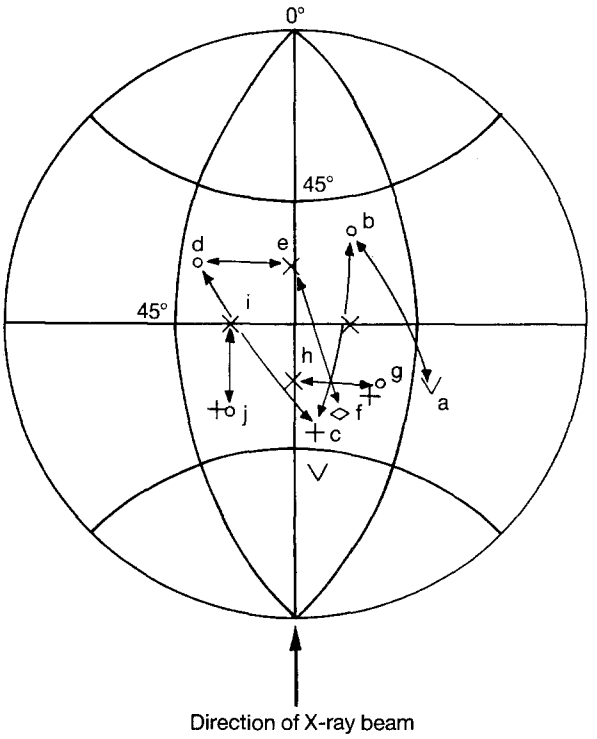

Figure 3 Stereographic projection of reciprocal-space spots found via X-ray diffraction studies. Spots belonging to hexagonal diamond show matching angular planes between a and b (58°), b and c (75°), c and d (75°), d and e (32°), e and f (62°), g and h (32°), and i and j (32°). (×) (0 0 2), (o) (1 0 3), (+) (1 1 0), (∨) (1 0 0), (◇) (1 0 1).

projection, the steric angles measured did not match those for a cubic lattice.

Nanocrystalline structures in the carbon film deposited on Si which could be assigned by matching X-ray diffraction angles to 2θ values and to angles between planes on the stereographic projection are listed in Table I. The peaks observed, with the crystal assignment for each observed peak, are shown in bold. It is important to note that the X-ray peak intensities corresponding to the (1 0 0) and (0 0 2) peaks of hexagonal diamond in the films are much more intense than the other peaks belonging to this crystal. This is

consistent with the original observations of Bundy and Kasper [1] concerning hexagonal diamond. The observed peaks belonging to the Si are not shown.

It can be argued that the observed angular relationships for reciprocal-space spots does not prove that diffraction is taking place from different planes in the same crystal (or a number of similarly oriented crystals), and that the "matching up" is coincidental. However, the constraint of a low grazing angle and the small number of reciprocal-space spots obtained, together with the fact that most of these spots can be given a value of 2θ as well as angular relationships in the stereographic projection, makes a strong case for the way in which the X-ray data have been interpreted, i.e. three distinct nanocrystalline structures in the films.

The size of the crystals in the films can be estimated by using the Scherrer formula

$$\Delta(2\theta) = \frac{0.9\lambda}{T\cos\theta}$$

where $\Delta(2\theta)$ is the full width half-maximum (FWHM) of the 2θ peak (in radians), λ the X-ray wavelength and T the particle size. The results for the crystal sizes calculated are shown in Table II. The two most intense peaks of each material found by X-ray diffraction were used to estimate the particle size in the films. The hexagonal diamond X-ray data are consistent with a crystal size of 20–30 nm. Hexagonal diamond crystals observed in the Canyon Diablo meteorite [1] as well as two recent reports of hexagonal diamond formation from a plasma source [8, 9] show crystal sizes in the range 10–50 nm. The crystals in these films were also present in the form of discontinuous clusters.

Raman studies of the films also show the existence of three different forms of carbon: a-C, graphite and hexagonal diamond. The Raman spectrum from the same film from which the X-ray data were obtained is shown in Fig. 4a. The characteristic broad G band of graphite centred around 1580 cm^{-1} is seen, together with the D band at 1355 cm^{-1} arising from the disorder present in microcrystalline graphite particles. Similar bands are also seen in films comprised mostly of a-C and/or a-C:H. The common Raman characteristic of a-C is a broad peak centred around 1550 cm^{-1}. The third Raman peak centred around 1170 cm^{-1} in Fig. 4a and b is consistent with that proposed for nanocrystalline diamond [13]. A similar Raman peak in the range 1130–1175 cm^{-1} [9, 14, 15] has been observed by others studying carbon films

TABLE II Crystal size derived from FWHM of X-ray peaks

d spacing (nm)	Crystal	FWHM (deg)	Particle size (nm)
0.218	Hex. diamond	0.31	27
0.206	Hex. diamond	0.28	30
0.334	Graphite	0.15	55
0.168	Graphite	0.20	45
0.161	SiC (4H)	0.25	36
0.142	SiC (4H)	0.25	40

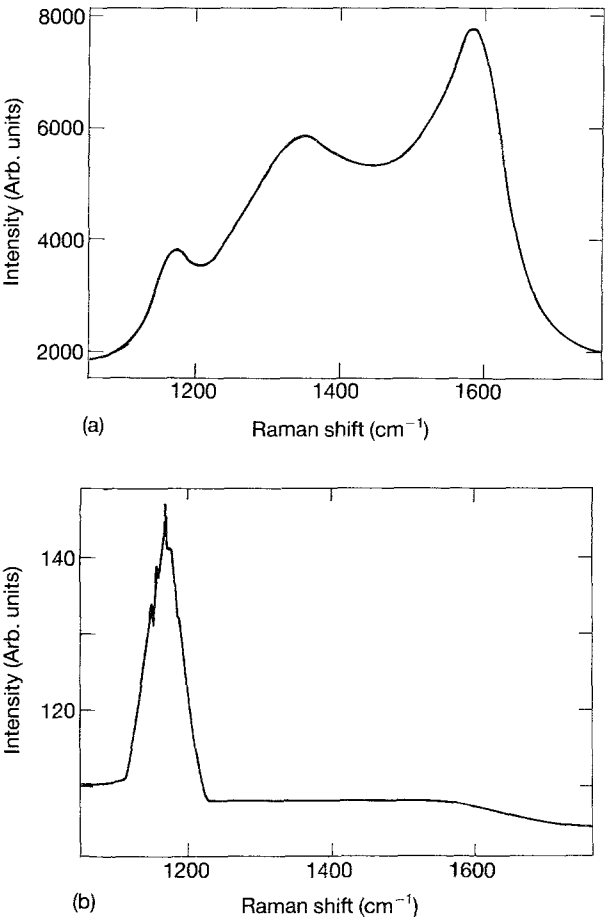

Figure 4 (a) Raman spectrum for a typical a-C film with both graphite and nanocrystalline diamond peaks at 1580, 1350 and 1170 cm^{-1}; (b) spectrum for an area which contains only the nanocrystalline hexagonal diamond peak at 1170 cm^{-1}.

and it is thought [16] that these peaks are also associated with a form of nanocrystalline diamond.

It is interesting to note that in the study of the Raman scattering in carbon by Nemanich *et al.* [16], they scaled the hexagonal SiC Raman modes and postulated that microcrystalline hexagonal diamond should give its strongest vibrational Raman frequency at 1175 cm^{-1}. This corresponds to the Raman peak observed in our films containing nanocrystalline hexagonal diamond, but without any evidence of microcrystalline cubic diamond. In the report by Maruyama *et al.* [9] on hexagonal diamond, a Raman response is shown at $\sim$1150 cm^{-1}, though they do not comment on its significance. The peaks ascribed to microcrystalline hexagonal diamond arises due to the micro-line Raman beam illuminating clusters of oriented hexagonal diamond crystals, the existence of which is confirmed by the directional X-ray peaks. A Raman spectrum from an area of the film which only shows the hexagonal diamond peak is shown in Fig. 4b.

Previous work on microcrystalline hexagonal diamond films formed under HTHP conditions reported by Knight *et al.* [17] did not show a peak at 1175 cm^{-1}. Their work reported a strong Raman mode at 1332 cm^{-1} identical to that seen in cubic diamond. A probable reason for the absence of the 1332 cm^{-1} peak is the fact that graphite has a scattering cross-section whose amplitude is 50 times greater than that of diamond, which would have

masked any diamond response. Another plausible reason for the absence of the 1332 cm^{-1} mode and the observation of the 1175 cm^{-1} peak is seen in the work of Wagner *et al.* [15]: in their work on diamond crystallites they showed that the Raman peak at 1332 cm^{-1} moves to values as low as 1100 cm^{-1} for 15–100 nm crystallites, depending on the frequency of the laser excitation source.

It has been proposed that when hexagonal diamond is produced by shock-loading graphite along its *c* axis, some of the graphite transforms itself to hexagonal diamond through a martensitic transition [18]. The presence of graphite in our samples suggests that hexagonal diamond may have formed by shock-compression of graphite particles due to energetic ion bombardment. For shock-compressed hexagonal diamond to form on oriented pyrographite at room temperature, pressures up to 25 GPa are needed [19]. It is also expected that with localized thermal spikes collapsing in 10^{-11} s an environment suitable for the formation of hexagonal diamond from suitably oriented graphite is available. Formation of hexagonal diamond in meteorites [2] is thought to be due to excessive pressure leading to a phase transformation. In low-temperature-deposited carbon films the phase transformation is also likely to be due to the excessive local pressure accompanying ion bombardment.

4. Conclusions

The results presented here together with other recent reports indicate that hexagonal diamond forms in plasma-deposited carbon films, though the mechanism by which this occurs is still not clear. The results show that three crystalline phases, hexagonal diamond, SiC and graphite, can be nucleated in a-C:H films deposited on Si from an r.f. plasma at low temperature and pressure. The Raman peak at 1170 cm^{-1} predicted analytically by Nemanich *et al.* [16] for nanocrystalline hexagonal diamond is also observed.

Acknowledgement

The authors express their thanks to Jane Southall of Newcastle Polytechnic for performing the Raman spectroscopy on these samples.

References

1. F. P. BUNDY and J. S. KASPER *J. Chem. Phys.* **46** (1967) 3437.
2. R. E. HANNEMAN, H. M. STRONG and F. P. BUNDY, *Science* **155** (1967) 995.
3. G. AMARATUNGA, A. PUTNIS, K. CLAY and W. MILNE, *Appl. Phys. Lett.* **55** (1989) 634.
4. M. SOKOLOWSKI and A. SOKOLOWSKA, *J. Cryst. Growth* **57** (1982) 185.
5. H. VORA and T. J. MARAVEC, *J. Appl. Phys.* **52** (1981) 6151.
6. S. R. P. SILVA, K. M. KNOWLES, G. A. J. AMARATUNGA and A. PUTNIS, *Diamond & Rel. Mater.* **3** (1994) 1048.
7. E. F. CHAIKOVSKI, V. PUZIKOV and A. SEMENOV, *Sov. Phys. Crystallogr.* **26** (1981) 122.
8. M. KITABATAKE and K. WASA. *J. Vac. Sci. Technol.* **A6** (1988) 1793.
9. K. MARUYAMA, M. MAKINO, N. KIKUKAWA and M. SHIRAISHI. *J. Mater. Sci. Lett.* **11** (1992) 116.
10. C. WEISSMANTEL, *Thin Solid Films* **92** (1982) 55.
11. M. J. BUERGER, "*Contemporary Crystallography*" (McGrawHill, New York, 1970) p. 137.
12. T. MORI and Y. MAMBA. *J. Appl. Phys.* **55** (1984) 3276.
13. W. A. YARBROUGH and R. ROY, "Diamond and diamond-like materials synthesis", edited by G. H. Johnson, A. R. Badzian and M. W. Geis (Materials Research Society, Pittsburgh, PA, 1988) p. 33.
14. P. BOU and L. VANDENBULCKE. *J. Electrochem. Soc.* **138** (1991) 2991.
15. J. WAGNER, C. WILD and P. KOILD. *Appl. Phys. Lett.* **59** (1991) 779.
16. R. J. NEMANICH, J. T. GLASS, G. LUCOVSKY and R. E. SHRODER. *J. Vac. Sci. Technol.* **A6** (1988) 1783.
17. D. KNIGHT and W. B. WHITE, *J. Mater. Res.* **4** (1989) 385.
18. A. V. KURDZUMOV, N. F. OSTROVSKAYA and A. N. PILYANKEVICH, *Sov. Powd. Metall. Metal Ceram.* **27** (1988) 34.
19. W. UTSUMI and T. YAGI, *Proc. Jpn Acad.* **67B** (1991) 159.

Received 15 February
and accepted 8 March 1994